Journal of Electrical Engineering, Electronics, Control and Computer Science – JEEECCS, Volume 7, Issue 25, pages 29-38, 2021

Analysis of Variable Frequency Drive Induction Motor Current Disturbances and Motor Redesign by Intelligent Optimization Techniques

Sunny Varghese John
Nagarjuna Fertilizers and Chemicals Limited
India

Kondapalli S. R. Rao, Rayapudi Srinivasa Rao
Jawaharlal Nehru Technological University
Kakinada, India

Abstract **– An analytical approach is presented in this paper to minimize the influence of disruptive current spikes occurring at low frequency operation in a Variable Frequency Drive (VFD) induction motor. The recorded test data of load current at low frequency of a high power induction motor coupled with a reciprocating pump in a process industry, is analyzed by Prony Analysis (PA) and Hilbert transform (HT). Optimal values of motor design parameters that deliver sufficient mechanical power at low frequency and cause the least disruptive current spikes is arrived at, by using intelligent optimization techniques like Artificial Bee Colony (ABC), Particle Swarm Optimization (PSO), Genetic Algorithm (GA) and Simulated Annealing (SA). Using the most optimal design values obtained, Taguchi method is applied on the VFD control parameters for getting minimal current spikes. The output of the Taguchi method is compared with the experimentally set value at site. The comparison proved that with the optimal design parameters of motor obtained from the optimization methods, are effective in being able to deliver stable operation of the motor at low frequency. The optimal motor design parameters derived in this paper can be used to procure a new motor that gives stable operation at low frequency.**

Keywords-Induction motor current spikes; Prony analysis; Hilbert transform; Taguchi's method; Artificial Bee Colony; Particle Swarm Optimization; Genetic Algorithm; Simulated Annealing

I. INTRODUCTION

In a process industry to achieve huge profits, the specific energy consumption is to be kept low. Almost all the industrial applications use VFDs to save on the energy. VFDs have advantages like - good range of speed control, soft start, deceleration and regeneration. Few disadvantages of the VFD are – drop in efficiency, harmonic generation in the system, and loss of torque at low frequencies. This paper addresses a serious problem encountered at low frequency operation of a 550 kilowatts VFD induction motor coupled to a reciprocating pump which transfers process critical and hazardous liquid ammonia in a Urea manufacturing fertilizer plant.

In a continuous process, there is a requirement sometimes to operate the system at low loads, due to limitations in the upstream section. During such occasions, it is financially beneficial to continue operating the process at low load than to stop and then resume back operations. But while trying to sustain low frequency operations, huge spikes in motor current and disturbances in the pumping speed and discharge pressure of the reciprocating pump is observed. These disturbances were observed to occur at random intervals and without warning. However when there was tripping of the drive causing sudden stoppage of ammonia flow at a high pressure of 236 kilograms per square centimeter, it raised serious safety concerns. It became very important to take effective action to prevent repeat of such safety incidents while also maintaining production stability at low frequency from profitability point of view. It was determined that the problem of spiking currents was due to the low torque developed at low frequency. The normally neglected resistance voltage drop, at higher frequencies, which is more pronounced at low frequency, is a reason for the low torque from the motor. In view of the requirement to keep operations going at low speeds, it became necessary to analyze the current spikes to obtain optimal control parameters for the drive as an immediate measure. And since the cost of disruption of process for even a single day could payback costs for procuring a new VFD and motor, it was worthwhile to invest on a new motor with optimally designed parameters to operate at the low frequencies required by the process.

Much effort has been made by researchers toward optimizing VFD induction motor parameters. [1] attempts to reduce current spikes levels using R-C filters in the gate control. An optimization-based tracking control method over the entire speed and torque range of an induction motor considering the nonlinear core saturation effects is researched in [2]. [3] compares two different induction motor control models indicating persistence of saturation during fault conditions. An experimentally validated study is made in [4] comparing two magnetic saturation induction motor models for designing voltage controllers. [5]

analyses induction motor with variable frequency drives considering issues of pulsating torque, distorted current and voltage waveforms, increasing losses etc. Genetic Algorithm is used in [6] to address an optimization problem with efficiency and active material cost as objective function. Researchers have mentioned about load current spikes of induction motor due to voltage transients that occur with variable frequency drives which switch the current rapidly and repeatedly. However the analysis on waveforms related to transient currents and current spikes is not investigated in their papers.

The main aim of this paper is to minimize the current spikes in a VFD induction motor when operating at low frequency and supplying a constant process control load through a reciprocating pump. This paper explores and proposes an analytical approach using Prony analysis (PA), and Hilbert Transform (HT) for analyzing the spike current signal and other intelligent optimization techniques like Artificial Bee Colony (ABC), Particle Swarm Optimization (PSO), Genetic Algorithm (GA), Simulated Annealing (SA) and Taguchi methods to redesign the motor and optimize the parameters of the motor and VFD.

Section 2 gives a brief description of the pump drive system and the adopted control scheme. Section 3 discusses load current signal analysis and intelligent optimization methods that are adopted in this paper. The performance tests on the motor and design analysis program are described in Section 4. Section 5 discusses the results and Section 6 presents the conclusions drawn.

II. PUMP DRIVE SYSTEM

The VFD used in the process under study is a microprocessor based pulse width modulated (PWM) digital controller and a current source inverter (CSI). The motor is a 550 kilowatts, 3-phase, 4-pole, 50 Hertz induction motor driving a reciprocating pump load. This setup is shown in Fig. 1.

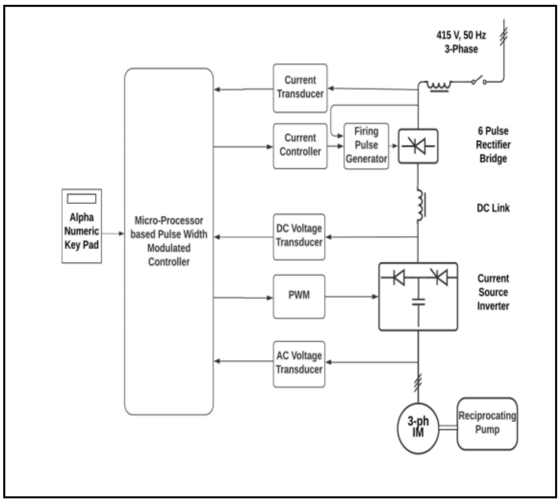

Figure 1: VFD 550 kW, 3-phase, 4-pole, 50 Hz induction motor

The CSI is fed through a variable dc link from a line side phase controlled rectifier. The motor current modulation ensures delivery of a smooth torque. In order to maintain constant air gap flux in the variable speed motor over the entire speed range, the voltage to frequency ratio is kept constant. Only at low frequencies it is required to increase the voltage slightly and thereby higher voltage to frequency ratio, to overcome the impedance voltage drop of motor. The drive parameters can be adjusted easily by using the alpha numeric key pad on the VFD panel [7].

III. OPTIMIZATION METHODS

A. Signal Analysis Methods

The application of power semiconductors in electrical drives, significantly distort the voltage and current waveforms. Hence the analysis of waveforms gains natural importance as a subfield. Many signal processing techniques exist for study and harmonic estimation. Fast Fourier Transform (FFT) is commonly used as it gives good estimation of harmonic spectrum of stationary and periodic signals. The magnitude of the spectrum gives details of the strength of the frequency components relative to other components while the phase gives information on the alignment of the frequencies in time. However, for short damped signals, due to limitations of FFT, other signal analysis methods are used.

This paper focuses on identifying the characteristics of the load current signal by two novel signal analysis methods viz., (i) Prony Analysis and (ii) Hilbert Transform. Prony analysis is a robust feature extracting method of fitting a linear combination of exponential terms to a signal [8]. The load current signal *f(t)* and its Hilbert transform *f^(t)* together create a strong analytic signal [9-11].

B. Prony Analysis

Prony Analysis (PA) is a high-resolution spectral analysis method and capable of accurately estimating the characteristics of the original waveform. It is a classical signal processing method, which extends the Fourier analysis and directly estimates the four key attributes of harmonics i.e. frequency, damping factor, amplitude, and relative phase of the signal, *y(t)*. Compared to FFT, PA is able to accurately fit the original slow and fast damping signals [12]. The sampled signal expressed as a linear combination of complex damped sinusoidal exponential terms is shown in (1) with magnitude A_i, the damping factor ζ_i, the frequency f_i, and the phase angle θ_i. Each exponential term with a different frequency is termed as mode of the signal. The signal, *y(t)* estimated by the Prony method is expressed as:

$$\boldsymbol{y(t) = \sum_{i=1}^{N} A_i\, e^{\xi it} cos(2\pi f_i t + \theta_i) \quad i = 1, 2, 3., N} \tag{1}$$

C. Hilbert Transform

Hilbert transform is another method to study the signal spectrum specifically its magnitude and phase characteristics as a function of frequency. By applying this method, complex components are separated from the signal. It is also used to obtain the minimum-phase response from a spectral analysis. In the time domain analysis, phase shift is done with the positive frequency constituents shifted by +90 degrees, and negative ones shifted by –90 degrees. A real function $f(t)$ and its Hilbert transform $f^{\wedge}(t)$ are related, together creating a strong analytic signal described with an amplitude and a phase. It helps to create an analytic signal based on the original real-valued signal and from which the instantaneous phase of the original signal is computed. The derivative of the phase gives the instantaneous frequency. The Fourier transform gives us a one-sided spectrum in the frequency domain whereas a function and its Hilbert transform also are orthogonal. Hilbert transform finds a companion function $f^{\wedge}(t)$ for a real function $f(t)$ such that $z(t) = f(t) + if^{\wedge}(t)$.

Hilbert transform of a signal can be obtained from the following steps. Calculate the Fourier transform of the given signal $f(t)$. Ignore the negative frequency signals. Calculate the inverse Fourier transform to get the Hilbert transform as a signal with complex values.

The characteristics of the signal $f(t)$ and its Hilbert transform $f^{\wedge}(t)$ have the same amplitude spectrum, autocorrelation function, energy spectral density. They are orthogonal and the Hilbert transform of $f^{\wedge}(t)$ is $-f(t)$. For any signal Hilbert transform exists, if its Fourier transform exists. The real and the imaginary parts of the transform are called a Hilbert-transform pair. When $f(t)$ is narrow-banded, $|z(t)|$ can be regarded as a slow-varying envelope of f(t) while the phase derivative $\partial t\ [tan^{-1}(y/x)]$ is an instantaneous frequency. Thus, Hilbert transform can be interpreted as a way to represent a narrow-band signal in terms of amplitude and frequency modulation.

D. Taguchi's Method

Taguchi, a Japanese engineer, designed an experimental optimization method to obtain a product of better quality. Optimization is realized by minimizing the deviation of the parameters from a target value. Taguchi method is based on orthogonal arrays. The orthogonal array matrix is designed to contain a combination of control parameters (CPs) and predefined levels for every control parameter. This design makes it possible for investigating the whole space with a limited number of experiments. An orthogonal matrix, Q satisfies the relation $Q^T = Q^{-1}$ [13-14].

Any process has several CPs that decide the target output. For the orthogonal matrix, every control parameter of the process is specified with certain levels within a recommended range which affect the per unit (p.u.) error of the target output [11]. For this paper, the selected number of levels $L = 5$, and control parameters $P = 6$, then the total number of experimental combinations possible are $N = L^P = 15625$. But, using L_{25} here, we need to conduct only 25 experiments for each level of control parameter independent of the values of other parameters [15-17]. The performance of the process is evaluated in several ways but here the p.u. error used and defined as $E_r = \|(T_{op} - A_{op})\| / \|T_{op}\|$, where T_{op} is the target output and A_{op} is the actual output.

The net effect of each level value in each factor is computed by averaging the results which contain the same level and factor. Finally, the levels indicating the least error are the best combination of control parameters.

E. Artificial Bee Colony (ABC) optimization technique

The ABC method, a population based optimization algorithm, is based on the intelligent behavior of foraging sister bees, working collectively, to collect nectar from flowers. These bees are broadly classified as employed foragers and unemployed foragers. Unemployed foragers are further classified as scouts and onlooker bees [18-20]. The division of labor in a colony is of three kinds: (i) employee bees, which work on collecting food at a specific site (ii) onlooker bees, which choose good food sites out of those located by the employed bees and (iii) scout bees, which seek new food locations at random. The employed foragers also carry back information about the distance, direction and site fitness to exchange it the colony's dance floor through a waggle dance. The onlooker bees collect the information from the dance pattern and go out to employee themselves at sites assessed as profitable. Scout bees are those that scout around at random for new sites.

Correlating this to an optimization problem, the source of nectar corresponds to a potential solution and the quantity of nectar to the quality of the solution. The artificial bees fly about in a multidimensional search space to locate the optimal solution. ABC employs three control parameters, namely, population size, maximum cycle number and convergence limit which are predetermined by the user. First, the optimization problem is converted to a problem of finding the best parameter vector that minimizes an objective function. After a random scouting to discover a population of initial solution vectors, the artificial bees move towards better solutions by local search methods, followed by global search, thereby, avoiding getting struck at local minima.

F. Particle Swarm Optimization (PSO)

The PSO algorithm, first proposed by James Kennedy and Russell Eberhart, in 1995, is based on the concept of swarm intelligence. The PSO is suitable for optimizing nonlinear continuous functions and complex optimization engineering problems. It takes its analogy from the social behavior of creatures like birds, fish etc., foraging for food or a place to settle. A swarm of birds flying overhead in a seemingly random fashion for a while, in the end, manage to land at a particular location. Actually, the decision of the final landing spot, is arrived at, based on various survival factors like availability of food, safety etc., and by an effective communication within the swarm [21]. The principles of PSO are self-organization, cooperation and an intelligent framework normally used when describing complex systems dynamics. Initially, a number of random particles are placed in the search area of the given optimization problem. Every particle has defining vectors like current position, previous best position and velocity. In an iteration step, the current position of the particle is reviewed as a potential solution called as Pbest, and it is compared not only with its previous Pbest position but also the group best which is called as Gbest. The step size of the iterations i.e. adjustment of the velocity vector, makes the particle move between its best and the global best positions according to (2) and (3). After a series of such iterations, the particles, depending on the number of iterations permitted, reach the global optimum [22-23].

$$V_i^{k+1} = W.V_i^k + C_1.rand_1.\left(Pbest_i - S_i^k\right) + C_2.rand_2.\left(Gbest_i - S_i^k\right) \quad (2)$$

$$X_i^{k+1} = X_i^k + V_i^{k+1} \quad (3)$$

where V_i^k is the current velocity of particle i at k^{th} iteration, V_i^{k+1} is the velocity (modified velocity) of particle at $(k+1)^{th}$ iteration, W is the inertia weight factor, C_1 and C_2 are the accelerating constants, $rand_1$ and $rand_2$ are random numbers between 0 and 1, $Pbest_i$ is the best value found by particle i until iteration k, $Gbest_i$ is the best particle found in the group until iteration, k, X_i^k is the current position of the particle, i at k^{th} iteration, X_i^{k+1} is the current position (modified searching point) of the particle i at $(k+1)^{th}$ iteration. The constants, C_1 and C_2 represent the weighting factors of the acceleration terms that pull each particle toward the *Pbest* and *Gbest* positions.

G. Genetic Algorithm (GA)

In evolutionary computation, a field of computational research, Genetic Algorithm (GA), is of prime importance. Invented by John Holland and based on the principles derived from natural evolution, the original intent was to formally study and use natural adaptation processes in the world of computers. The study opened doors to a powerful optimization technique in GA. The principles of evolution adopted in GA are quite simple: species evolve by random variation i.e. crossover, mutation etc. The fittest ones, by reproduction, transfer genetic property. GA primarily utilizes search spaces, populations of chromosomes, selection of fittest ones, crossover, and mutation of new offspring [24-25]. For a given optimization problem, the GA starts with n chromosomes - a random sized population each of a specified bit length. Each chromosome is a potential solution and the fitness of each chromosome is calculated. Pairs of chromosomes are crossed over at randomly chosen points to form two offspring. The probability of the pairs chosen, are according their fitness. The offspring which are then mutated at each locus are placed in the new population. In GA, an iteration called generation is again executed with the newly formed offspring population. The optimal or fittest solution is arrived at, after a run which consists of many generations.

H. Simulated Annealing Optimization Technique

Annealing is a process where a solid material is heated up and then allowed to cool down slowly to alter its physical properties. As the hot solid cools down slowly to its final state, it passes through various stages each stage with its own energy value. In the final state the material internal structure is altered and retains properties different from the original. The analogy of this physical process of annealing is compared with the iterative process of obtaining an optimal solution among a number of likely solutions to an optimization problem. The various stages of cooling are analogous to possible solutions and the energy state of the particular stage is analogous to a value of objective function calculated at that solution. The least or minimum energy state gives the optimal solution to the problem. The algorithm has a number of iterative steps and each step changes the solution of that iteration to obtain a new solution. The convergence to the optimal solution is governed by a cooling schedule, specified by an initial value of the control parameter (i.e. temperature), a decrement function for lowering the value of the control parameter, a final value of the control parameter specified by a stop criterion and a finite length of each homogeneous Markov chain [26-27].

The algorithm evaluates the neighboring states of the problem, which are actually new states derived through carefully modifying a given state. The defined way of altering a state to produce neighboring states is called a move and each move further gives different sets of neighboring states. An acceptance probability function decides on whether to transit from the current state to a possible new state. This depends on the energies of the two states, and on a global time-varying parameter called the temperature. States with a smaller energy are better than those with a greater energy. The probability function must be positive even when the energy of the new state is greater than previous one. This prevents the algorithm from getting stuck at an energy state worse the global one. Initially the iterations make a broad use of the search space, scanning through good solutions overlooking smaller features of the energy function and then move toward the narrower space of low-energy regions to the final global optimal solution.

IV. EXPERIMENTAL TESTS ON VFD INDUCTION MOTOR

Experimental tests were carried out on VFD induction motor coupled to a reciprocating pump for controlled fluid flow to study the effect of stator current spikes at the lowest pumping speed expected at low plant loads.

TABLE I. LOAD TEST SETTINGS ON 550 KW VFD INDUCTION MOTOR

Voltage, U	**Frequency, Hz**	***U/f* ratio**	**Power Input, kW**
248.79	30	8.29	233.31
255.80	30	8.52	239.89
260.49	30	8.68	244.29
273.1	30	9.1	256.02

At the corresponding frequency of 30 Hertz, tests are carried out with four different voltage and *U/f* settings as listed in Table I. At the first setting with voltage 248.79 volts and U/f ratio 8.29, the running current of the motor was stable at 636 A for a while before it shot up suddenly with a current spike up to 833 A by the 9th second, and then gradually increasing to about 1310 A by the 14th second. In another 5 seconds, the drive tripped.

The actual recorded time variation of stator current and pump pressure over a period of 35 seconds with the first setting of Table I is shown in Table II and graphically reproduced in Fig. 2.

TABLE II. TIME VARIATION OF STATOR CURRENT AND PUMP PRESSURE

Time Sec.[a]	Amps A[b]	Disc. Press. kg/cm^2.[c]	Time Sec.[a]	Amps A[b]	Disc. Press. kg/cm^2.[c]
0	636.0	236.6	18	1314.5	203.7
1	637.1	236.6	19	1279.5	208.2
2	636.8	236.6	**20**	**1233.0**	**211.5**
3	636.2	236.6	21	677.6	214.1
4	637.5	236.6	22	339.7	214.4
5	637.0	236.5	23	170.5	209.9
6	636.8	236.6	24	85.9	202.3
7	637.3	236.6	25	43.6	193.3
8	636.2	236.6	26	22.4	184.1
9	**833.9**	**236.6**	27	11.7	175.1
10	1082.3	233.8	28	6.5	166.5
11	1220.9	227.5	29	3.8	158.5
12	1290.1	218.6	30	2.4	151.1
13	1313.8	208.4	31	1.8	144.2
14	1305.7	198.0	32	1.5	137.8
15	1310.2	190.3	33	1.2	131.8
16	1310.9	190.7	34	1.1	126.1
17	1312.7	197.7	35	1.1	120.8

a. Sec is seconds,

b. Amps is the motor amperage

c. Disc. Press. is the pump discharge pressure in kg/cm^2

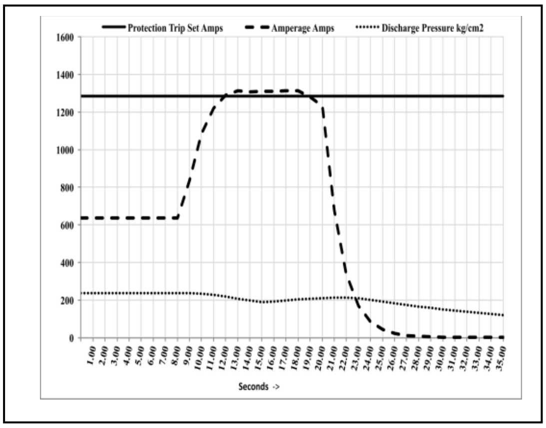

Figure 2: Variation in stator current at V/f = 8.29

From the recorded current data, a closed form equation, ct(t), is derived by using a computer program and represented by (4).

$$ct(t) = 636.583 + 0.017t + 308.269e^{0.108t} +1274.078003 + 2.16982t +3557253.75e^{-0.424203t} \quad (4)$$

With Eq. (4) as the input signal for PA, the Prony terms are derived by MATLAB code. Figs. 3a to 3d represent the plots for amplitude A_i, the damping factor ζi, the frequency f_i, and the phase angle θ_i over a time period of 20 sec.

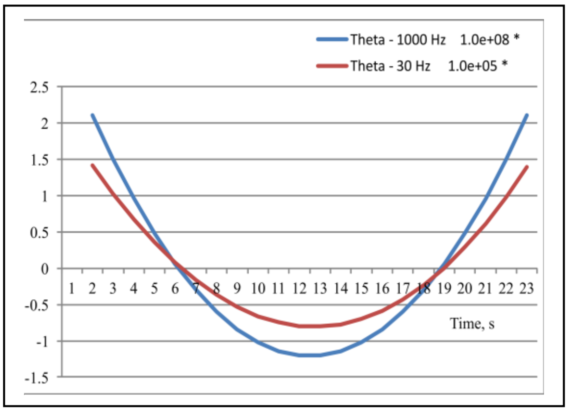

Figure 3a. Prony terms - Phase angle versus time

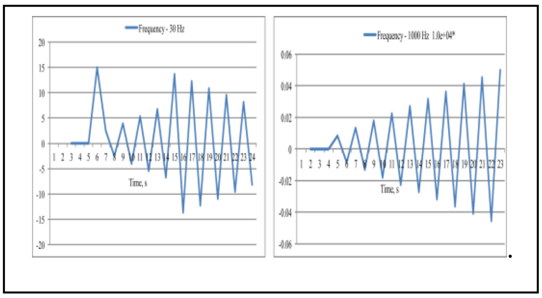

Figure 3b. Prony terms - Frequency versus time at 30 Hz, 1000 Hz

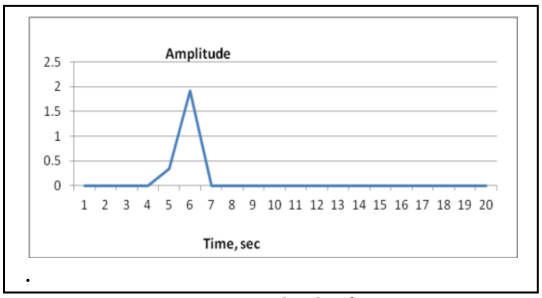

Figure 3c. Prony terms - Amplitude of current versus time

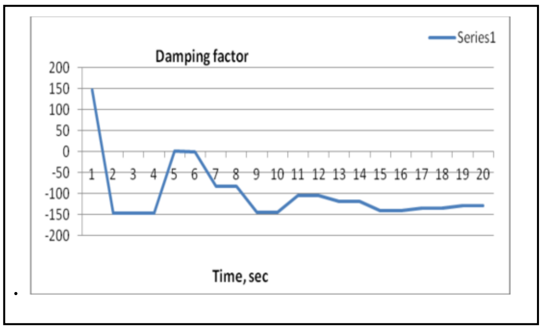

Figure 3d: Prony terms - Damping factor versus time

In order to extract the characteristics of load current signal by Hilbert Transform at two different sampling frequencies a MATLAB code is developed. Figs. 4a and 4b represent modulated signal, the extracted envelop and the extracted carrier. The regenerated carrier is often referred as Temporal Fine Structure (TFS).

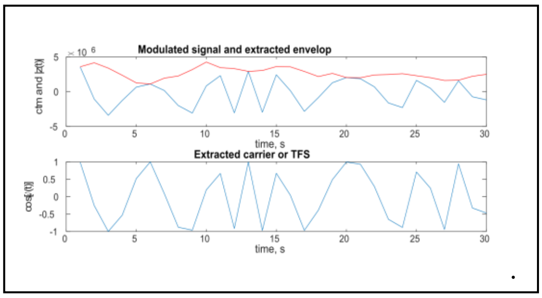

Figure 4a. Sampling frequency 30 Hz - Modulated signal and extracted envelope and TFS

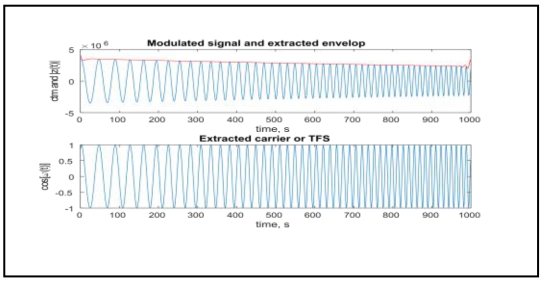

Figure 4b. Sampling frequency 1000 Hz - Modulated signal and extracted envelope and TFS

At the second and third settings of voltage and voltage to frequency ratio of Table I, high current spikes were observed and they caused process disturbances. However, there was no trip. But for the fourth voltage setting, when the voltage to frequency ratio was increased to 9.10, the system performed much better without either abnormal current spikes or process disturbances. This is shown in Fig. 5.

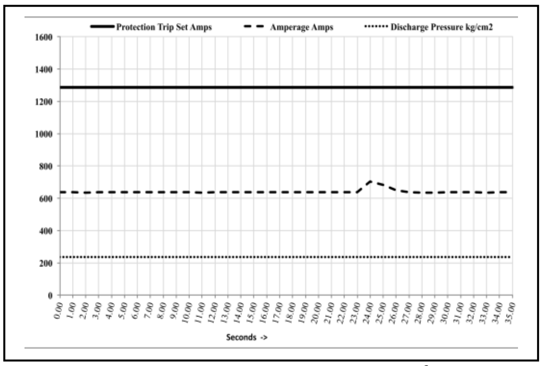

Figure 5. Variation in stator current at V/f = 9.1

Based on the investigations, it could be concluded that the problem of maximum current spike and consequent drive trip was due to the low torque and large stator resistance voltage drop developed by the motor at low frequency. The torque could be boosted by increasing the input voltage keeping the frequency constant at 30 hertz.

V. Results and Discussion

To achieve high performance varying speed operation of the motor, it is proposed in this paper to redesign the motor parameters with spike current as one of the design variables. For the design analysis of the induction motor, together with optimization techniques, a C/C++ program is developed considering 18 design variables and 33 constraints. This mathematical model is developed as a non-linear programming (NLP) problem. In addition to the motor performance constraints such as maximum mechanical power output, efficiency etc., all the 18 design variables are constrained with lower and upper bounds based on the actual parameters of the motor to satisfy the objective function which is the permissible stator current without current spikes. In addition, the program computes many performance values of the induction motor such as efficiency, maximum mechanical power, torque developed, power developed, losses etc., based on equivalent circuit at 30 hertz frequency operation and is flexible to minimize any performance value as objective function.

TABLE III. Optimal design parameters of the 3-phase 550 kW induction motor

Design parameter	ABC	PSO	GA	SA
x_1 - Diameter of the stator bore, mm	353.30	429.50	371.84	450.00
x_2 - Length of the stator core, mm	438.10	429.40	406.81	400.00
x_3 - Width of the stator slot, mm	12.50	13.20	12.16	10.00
x_4 - Depth of the stator slot, mm	75.00	79.30	70.99	85.00
x_5 - Depth of the stator core, mm	119.80	137.90	118.60	110.00
x_6 - Air gap length, mm	2.90	2.70	2.52	3.00
x_7 - Width of rotor slot, mm	7.30	7.30	7.94	7.20
x_8 - Depth of rotor slot, mm	44.20	51.70	45.65	40.00
x_9 - Depth of rotor core, mm	107.40	102.80	114.98	130.00
x_{10} - Average flux density in the air gap, T	0.75	0.73	0.74	0.70
x_{11} - Area of cross section of end ring, mm2	2138.8	2143.5	2107.2	2100.4
x_{12} - Stator current density, A/mm2	3.36	3.04	3.12	3.00
x_{13} - Spike current, A	401.05	401.98	406.43	409.54
x_{14} - Voltage, U	276.65	271.83	275.58	272.94
x_{15} - U/f ratio	9.11	9.11	9.08	9.15
x_{16} - Power input, kW	255.23	250.71	255.10	255.04
x_{17} - Pump discharge pressure, kg/cm2	232.36	236.97	234.50	233.44
x_{18} - Pump efficiency	0.75	0.73	0.74	0.75

The NLP problem is stated as: Find the design variables (x_1 to x_{18}) = X, such that $F(X)$, a nonlinear objective function is a minimum, subject to the nonlinear constraint functions, $g_j(X)\{\leq=\}0$, $j = 1, 2, \ldots$

m with $X \le 0$ being a non-negative solution. An augmented objective function, P is formulated by using exterior penalty function method as:

$$P(X,r) = F(X) + r\sum_{i=1}^{N}\left[g_j(X)\right]2,\ r \ge 0 \qquad (5)$$

where *r* is the penalty factor [28].

The optimal motor design variables obtained by using the ABC, PSO, GA and SA optimization techniques to minimize the spike current are presented in Table III, by keeping a constant frequency of 30 Hertz and load test settings as in Table I, item 4.

It is seen that the optimal design parameters of the motor derived by ABC method gives the best efficiency and lowest spike current. Having obtained the optimal motor design parameters, the next step is to develop the L_{25} Taguchi matrix to compute the optimal combination of process control parameters. The optimal values of the spike current, voltage, voltage to frequency ratio, pump efficiency, power input, and process pump discharge pressure are considered as the six control parameters for the Taguchi table. For each of the control parameters, an appropriate band which encloses the values obtained are considered. They are evenly spaced for consideration as levels of the Taguchi table and are presented in Table IV.

TABLE IV. CONTROL PARAMETERS FOR TAGUCHI TABLE

Sn	A[a]	B[b]	C[c]	D[d]	E[e]	F[f]
1	270 (1)	9.08 (1)	0.72 (1)	399 (1)	249 (1)	232 (1)
2	272 (2)	9.10 (2)	0.73 (2)	402 (2)	251 (2)	233 (2)
3	274 (3)	9.12 (3)	0.74 (3)	405 (3)	253 (3)	234 (3)
4	276 (4)	9.14 (4)	0.75 (4)	408 (4)	255 (4)	235 (4)
5	278 (4)	9.16 (5)	0.76 (5)	411 (5)	257 (5)	236 (5)

a. A is the motor input voltage in volts
b. B is the voltage to frequency ratio
c. C is the pump efficiency
d. D is the spike current, in amperes
e. E is the motor power input P_{in} in kW.
f. F is the pump discharge pressure P_{dis} in kg/cm^2

These six process control parameters and levels are used to conduct the Taguchi experiments. The corresponding levels for each of these 6 control parameters are shown in Table V. A simulation program is run to compute the pump output power in kilowatts, P_{sop}, from each set of process control parameters from each of the 25 experimental steps of Taguchi matrix. The results are listed in column 8 of Table V. The next step is to compute the error in pump outputs from the simulation program and the actual pump operation.

Considering the actual fluid flow parameters of the process, the pump actual out power in kilowatts, P_{aop}, is determined from the following expressions:

The volumetric flow rate at a given pump speed is expressed as:

$$V_{fr}=V_{mf}.N_f/V_{fr} \qquad (6)$$

where V_{mf} is the maximum rated pump flow in m^3/hr, N_f is the speed in rpm at the operating frequency *f*, and N_{ms} is the pump maximum rated speed in rpm.

TABLE V. TAGUCHI'S EXPERIMENTS AND CORRESPONDING ESTIMATED ERROR

Sn	A[a]	B[b]	C[c]	D[d]	E[e]	F[f]	G[g]	H[h]	p.u. Error
1	1	1	1	1	1	1	119.24	195.61	0.39044
2	1	2	2	2	2	2	118.71	196.54	0.39601
3	1	3	3	3	3	3	118.19	197.48	0.40150
4	1	4	4	4	4	4	117.67	198.42	0.40693
5	1	5	5	5	5	5	117.16	196.14	0.40265
6	2	1	2	3	4	5	121.01	199.35	0.39299
7	2	2	3	4	5	1	120.48	195.61	0.38409
8	2	3	4	5	1	2	119.95	196.54	0.38971
9	2	4	5	1	2	3	119.42	197.48	0.39526
10	2	5	1	2	3	4	118.90	198.42	0.40074
11	3	1	3	5	2	4	122.79	201.62	0.39095
12	3	2	4	1	3	5	122.25	202.57	0.39648
13	3	3	5	2	4	1	121.72	198.76	0.38762
14	3	4	1	3	5	2	121.19	196.54	0.38341
15	3	5	2	4	1	3	120.66	197.48	0.38901
16	4	1	4	2	5	3	124.59	200.67	0.37910
17	4	2	5	3	1	4	124.05	201.62	0.38474
18	4	3	1	4	2	5	123.50	202.57	0.39032
19	4	4	2	5	3	1	122.96	198.76	0.38136
20	4	5	3	1	4	2	122.43	199.71	0.38699
21	5	1	5	4	3	2	126.41	202.88	0.37696
22	5	2	1	5	4	3	125.85	203.85	0.38263
23	5	3	2	1	5	4	125.30	204.82	0.38824
24	5	4	3	2	1	5	124.75	202.57	0.38415
25	5	5	4	3	2	1	124.21	198.76	0.37510

a. A is the motor input voltage in volts
b. B is the voltage to frequency ratio
c. C is the pump efficiency
d. D is the spike current, in amperes
e. E is the motor power input in kW, P_{in}.
f. F is the pump discharge pressure in kg/cm^2, $P_{dis.}$
g. G is the pump output power in kW, $P_{sop.}$
h. H is the actual pump output power in kW, P_{aop}.

Considering the resultant pump pressure P_r expressed in Pascal (1 kg/cm^2 = 98066.5 Pa) which is the difference between the pump input pressure and the output pressure and based on the volumetric fluid flow rate, V_{fr} measured in m^3/hr, the pump actual output power, P_{aop}, is computed as:

$$P_{aop} = (V_{fr}.P_r)/(3600.1000) \quad (7)$$

These calculated practical pump actual output powers are listed as shown in column 9 of Table V. The p.u. error in output powers of the pump is estimated as:

$$E_r = |(P_{sop} - P_{aop})/P_{sop}| \quad (8)$$

The p.u. error, E_r computed from the pump outputs for each experimental run is shown in the last column of Table V.

The permissible and safe spike phase current range of 400 A to 408 A considered in the Taguchi table is based on limiting it to a shoot up current of 33 A to 41 A over 367 A which is the normal phase current. In line current terms it means a shoot up of 57 A to 71 A over 636 Amps, which is practically acceptable.

The net effect of each level value in each factor is computed by averaging the results which contain the same level and factor. Table VI shows the net effect and average of each CP and each level as mentioned above.

TABLE VI. AVERAGE OF EACH CP AND EACH LEVEL

	Level of control parameters				
CPs	**1**	**2**	**3**	**4**	**5**
Motor input voltage V	0.3995	0.3926	0.3895	0.3845	**0.3814**
Voltage to frequency ratio *V/ f*	**0.3861**	0.3888	0.3915	0.3902	0.3909
Pump efficiency	0.3895	0.3915	0.3895	0.3895	**0.3894**
Spike current A	0.3915	0.3895	0.3894	**0.3875**	0.3895
Motor power input in kW	0.3876	0.3895	0.3914	0.3914	**0.3875**
Pump discharge pressure kg/cm^2	**0.3837**	0.3866	0.3895	0.3943	0.3933

From the Taguchi results in Table VI we see that the optimal combination of parameters with smallest effective error is 5, 1, 5, 4, 5, 1 and the corresponding values of CPs settings are (refer to Table IV) - voltage in volts is 278, voltage to frequency ratio is 9.08, pump efficiency is 0.76, spike phase current in amperes is 408.00, power in kilowatts is 257, and discharge pressure in kilograms per square centimeter is 232, which give stable operation of the motor. From the Taguchi results we see that voltage to frequency ratio is 9.08 and from the practical results the voltage to frequency ratio is 9.10. The comparison shows that the VFD induction motor would require only a lower voltage to frequency ratio setting with the proposed optimized motor design and VFD control parameters thereby validating the method.

In other words the motor designed by the optimization method can be operated at a lower voltage to frequency ratio than the present working motor.

In this proposed methodology, by choosing a wider spike current band as objective function in the optimizations we can obtain an optimized motor design that can operate at even lower voltage to frequency ratio without causing process disturbance or trip.

ACKNOWLEDGMENTS

The authors gratefully acknowledge the support provided by Jawaharlal Nehru Technological University Kakinada, Kakinada, India and Nagarjuna Fertilizers and Chemicals Limited, Kakinada, India.

CONCLUSIONS

In process industries, VFDs are used to reduce specific energy consumption. However serious disadvantages are seen when the process is required to operate at low frequencies. In a high power 3-phase induction motor coupled with a reciprocating pump of ammonia transfer service at high pressure and driven by a VFD, there were occurrences of huge spiking of current followed by disruption of the process. This was mainly because of the low torque developed by the motor at low frequency operation. It was very important to address these instances for safety concerns primarily and for profitability. This paper proposes an approach to minimize the current spikes, occurring at low frequency. Based on the recorded data of load current, feature extraction and characteristics are analyzed by two novel signal analysis methods viz., PA and HT. Optimization techniques - ABC, PSO, GA and SA are used to redesign the motor considering current spikes minimization as the objective function. Taguchi method is then used to get optimal control parameters of the VFD. The proposed methodology is validated by comparing with the experimental steps and practical operation of the motor. As the cost of disruption of process for a single day could well pay twice over for a totally new VFD and motor, the new design can be used when procuring a new motor which can operate at specific low frequencies.

NOMENCLATURE

$\partial t\ [tan^{-1}(y/x)]$	Phase derivative is an instantaneous frequency
ABC	Artificial Bee Colony
A_i	Signal magnitude
Amps	Motor amperage
A_{op}	Actual output
C_1 and C_2	Accelerating constants or weighting factors of the acceleration terms
CPs or P	Control parameters
CSI	Current source inverter
ct(t)	Closed form equation of recorded current data, a closed
Disc. Press.	Pump discharge pressure in kg/cm^2
E_r	Per unit error
f	Operating frequency

f(t)	Real function
F(X)	Nonlinear objective function.
f^(t)	Hilbert transform of f(t)
FFT	Fast Fourier Transform
f_i	Signal frequency
GA	Genetic Algorithm
Gbest	Group best
Gbesti	Best particle found in the group until iteration, k
$g_j(X)$	Nonlinear constraint function
HT	Hilbert transform
Hz	Frequency in Hertz
kg/cm^2	Kilogram per square centimeter
kW	Power Input in kilowatts
L	Number of levels
m^3/hr	Cubic meter per hour
mm^2	millimeter squared
N	Number of experimental combinations
N_f	Speed in rpm
NLP	Non-linear problem
N_{ms}	Pump maximum rated speed in rpm
P	Penalty function
p.u.	Per unit
PA	Prony Analysis
P_{aop}	Actual pump output power
Pbest	Previous best
Pbesti	Best value found by particle i until iteration k
P_{dis}	Pump discharge pressure in kg/cm^2
P_{in}	Motor input voltage
PSO	Particle Swarm Optimization
P_{sop}	Computed or simulated pump output power
PWM	Pulse width modulated
Q	Orthogonal matrix
r	Penalty factor
rand1, rand2	Random numbers between 0 and 1
SA	Simulated Annealing.
Sec	Seconds
t	Time in seconds
T	Tesla
TFS	Temporal Fine Structure (Regenerated carrier)
T_{op}	Target output
U	Voltage
U/f	Voltage upon frequency ratio
VFD	Variable Frequency Drive
V_i^k	Current velocity of particle i at k^{th} iteration
V_i^{k+1}	Modified velocity of particle at $(k+1)^{th}$ iteration
V_{mf}	Maximum rated pump flow in m^3/hr
W	Inertia weight factor
X	Design variable
x_1	Diameter of the stator bore, mm
x_2	Length of the stator core in mm
x_3	Width of the stator slot in mm
x_4	Depth of the stator slot in mm
x_5	Depth of the stator core in mm
x_6	Air gap length in mm
x_7	Width of rotor slot in mm
x_8	Depth of rotor slot in mm
x_9	Depth of rotor core in mm
x_{10}	Average flux density in the air gap, T
x_{11}	Area of cross section of end ring in mm^2
x_{12}	Stator current density in amperes per mm^2
x_{13}	Spike current in amperes
x_{14}	Voltage in volts
x_{15}	*U/f* ratio
x_{16}	Power input in kW
x_{17}	Pump discharge pressure in kg/cm2
x_{18}	Pump efficiency
X_i^k	Current position of the particle, *i* at k^{th} iteration
X_i^{k+1}	Current position (modified) of the particle *i* at $(k+1)^{th}$ iteration
y(t)	Signal
z(t)	Slow-varying envelope of *f(t)*
ζ_i	Signal damping factor
θ_i	Signal phase angle

REFERENCES

[1] D. Mohamed, S. Doubabi, and A.Rachid, “Current Spikes Minimization Method for Three-Phase Permanent Magnet Brushless DC Motor with Real-Time Implementation”, Energies, 11(11), 2018, pp.1-14.

[2] R. Tarvirdilu-Asl, S. Nalakath, Z. Xia, Y. Sun, J. Wiseman and A. Emadi, "Improved Online Optimization-Based Optimal Tracking Control Method for Induction Motor Drives”, IEEE Transactions on Power Electronics, 35, 2020, pp. 10654-10672.

[3] F. S. El-Faouri, O. Mohamed, and W. A. Elhaija, “Comparison of Three-Phase Induction Motor Control Models Incorporating Mutual Flux Saturation Effect”, International Journal on Energy Conversion, 5(5), 2017:135.

[4] O. Kiselychnyk, M. Bodson, and J. Wang, Comparison of two magnetic saturation models of induction machines and experimental validation, IEEE Transactions on Industrial Electronics, 64(1), 2017, pp. 81-90.

[5] D. Kumar, “Performance Analysis of Three-Phase Induction Motor with AC Direct and VFD”, IOP Conference Series: Materials Science and Engineering, 2018, pp. 1-10.

[6] R. Chaudhary, A. Shahpatel and S. Patel, Optimal design of Induction Motor using Genetic Algorithm and comparision with conventionally Designed Induction motor, IEEE 1st International Conference on Power Electronics, Intelligent Control and Energy Systems, Delhi, 2016, pp.1-4.

[7] Ansaldo Industria BMB Elettronica Industriale s.p.a., Current source dc link converter series, Silcovert AD (operating manual).

[8] L. Qi, L. Qian, S. Woodruff, and D. Cartes, "Prony analysis for power system transient harmonics", EURASIP J. Adv. Signal Process., 2007.

[9] M. Johansson, "The Hilbert transform", Master Thesis of Mathematics / Applied Mathematics, Växjö University, March 1999.

[10] Y.Lei, “Signal processing and feature extraction”, Intelligent Fault Diagnosis and Remaining Useful Life Prediction of Rotating Machinery, Butterworth-Heinemann, 2017, pp. 17-66

[11] B. Saddam, A. Aissa, B. S. Ahmed and S. Abdellatif, "Detection of rotor faults based on Hilbert Transform and neural network for an induction machine", 5th International Conference on Electrical Engineering-Boumerdes (ICEE-B) Boumerdes, 2017, pp. 1-6.

[12] F. D. Zahlay, and K. S. R. Rao, "Neuro-prony and Taguchi's methodology-based adaptive autoreclosure scheme for

electric transmission systems", *IEEE Trans. Power Del.*, vol. 27, no. 2, Apr. 2012, pp. 575-582.

[13] A. Sorgdrager, R. Wang, and A. J. Grobler, "Taguchi Method in Electrical Machine Design", SAIEE Africa Research Journal, 108 (12), 2017, pp. 150-164.

[14] H. R. Lochner, Designing for quality - An introduction to the best of Taguchi and western m ethods of statistical method design, (Chapman and Hall), 1990.

[15] Z. F. Desta, K. S. Ramarao, and T. B. Ibrahim, A new intelligent auto-reclosing scheme using artificial neural network and Taguchi's methodology, IEEE Transactions on Industry Applications, 47(1), 2010, pp. 306-313.

[16] J. M. Cimbala, Taguchi orthogonal arrays, Penn State University, Latest revision, 2014.

[17] K. L. N. Murthy, B. Sandeep, R. Vanukuru, and T. Chaitanya, A Review on Taguchi's Technique of forming Orthogonal Arrays. Journal of Advances in Mechanical Engineering and Science, 3(6), 2017, pp. 9-14.

[18] D. Karaboga. An idea based on honey bee swarm for numerical optimisation. Technical Report, Computer Engineering Department, Erciyes University, Kayseri, Turkey, 2005.

[19] D. Karaboga, B. Gorkemli, C. Ozturk, and N. Karaboga, "A comprehensive survey: Artificial bee colony (ABC) algorithm and applications," Artificial Intelligence Revolution, vol. 42, no. 1, Jun. 2014, pp. 21–57.

[20] P. P. Das and S. N. Mahato, "Artificial Bee Colony based design optimization of a six-phase induction motor," 2016 2nd International Conference on Control, Instrumentation, Energy & Communication (CIEC), Kolkata, 2016, pp. 526-530

[21] B. Almeida and V. Coppo, Particle Swarm Optimization: A Powerful Technique for Solving Engineering Problems, 2019, 10.5772/intechopen.89633.

[22] J. Kennedy, and R. Eberhart, Particle swarm optimization, in: Neural Networks, 1995. proceedings., IEEE International Conference on, Vol. 4, 1995, pp. 1942–1948.

[23] Mason, Karl; Duggan, Jim; Howley, Enda (2017). "Multi-objective dynamic economic emission dispatch using particle swarm optimisation variants". Neurocomputing. 270: 188–197. doi:10.1016/j.neucom.2017.03.086

[24] J. H. Holland, Adaptation in natural and artificial systems, Ann Arbor MI: The University of Michigan Press, 1975.

[25] H. Lingaraj, "A Study on Genetic Algorithm and its Applications", International journal of computer sciences and engineering, 2016, 4(10):139-143

[26] L. Wang and Y. Liu, "Application of Simulated Annealing Particle Swarm Optimization Based on Correlation in Parameter Identification of Induction Motor", Mathematical Problems in Engineering, 7, 2018, pp. 1-9.

[27] F. Busetti . Simulated annealing overview, 2003.

[28] P. D.Moral, A. Doucet, A. Jasra. Sequential Monte Carlo samplers. Journal of the Royal Statistical Society, Series B. 68 (3), 2006, 411–436.